AD 700 441
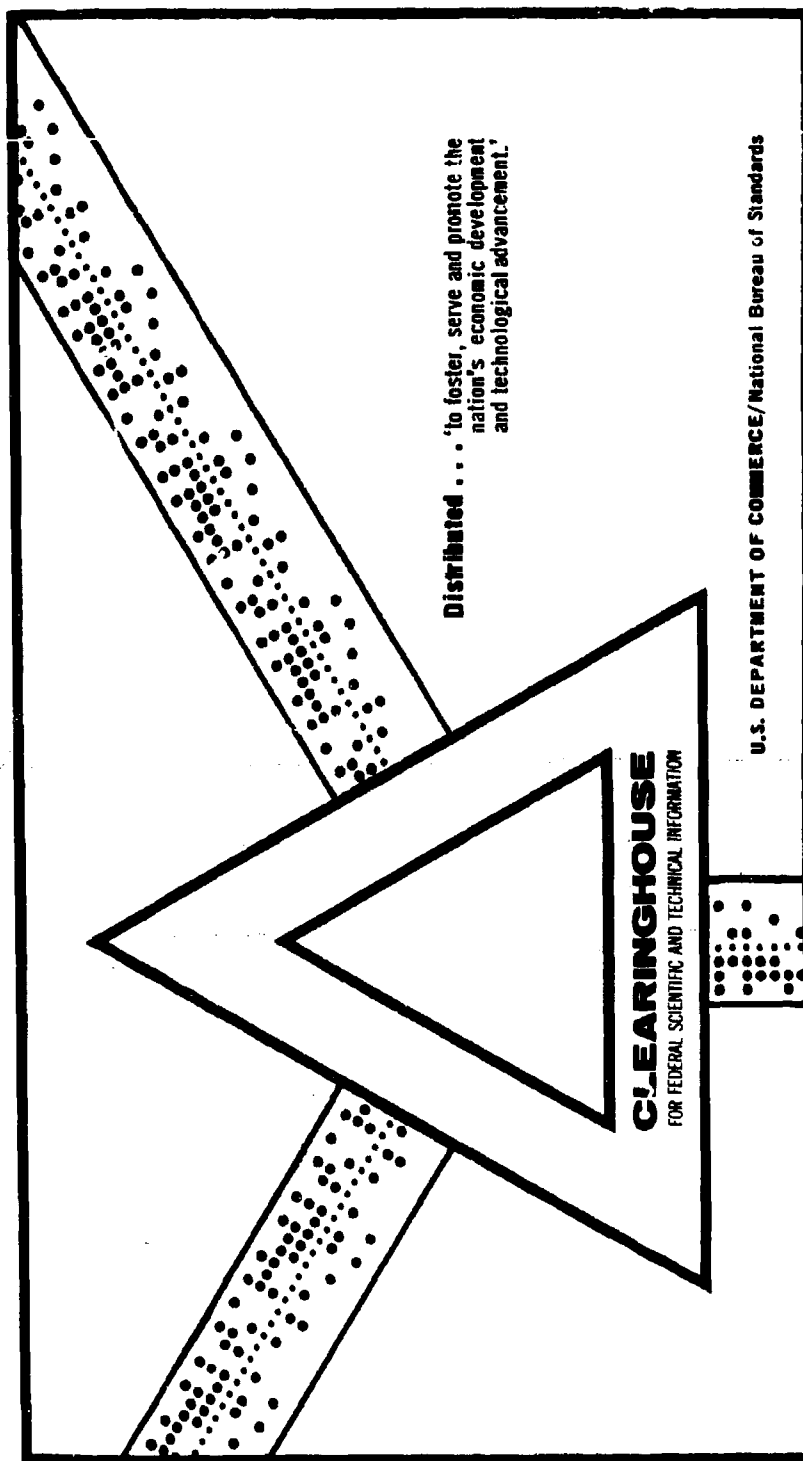
THE ELECTRODELESS SPARK UNDERWATER SOUND SOURCE

H. A. Wright, Jr.

Avco Government Products Group
Lowell, Massachusetts

8 January 1970

CLEARINGHOUSE
FOR FEDERAL SCIENTIFIC AND TECHNICAL INFORMATION

Distributed . . . "to foster, serve and promote the nation's economic development and technological advancement."

U.S. DEPARTMENT OF COMMERCE/National Bureau of Standards

SUMMARY TECHNICAL REPORT
THE ELECTRODELESS SPARK UNDERWATER
SOUND SOURCE

AVATD-0200-69-RR
Contract Nonr 4389(00)

8 January 1970

D D C

FEB 12 1970

D

Prepared for

CODE 468
OFFICE OF NAVAL RESEARCH
DEPARTMENT OF THE NAVY
Washington, D.C.

Prepared by

AVCO APPLIED TECHNOLOGY DIVISION
AVCO GOVERNMENT PRODUCTS GROUP
Lowell Industrial Park
Lowell, Massachusetts 01851

39

SUMMARY TECHNICAL REPORT
THE ELECTRODELESS SPARK UNDERWATER
SOUND SOURCE

AVATD-0200-69-RR
Contract Nonr 4389(00)

by

H. A. Wright, Jr.

8 January 1970

ABSTRACT

The electrodeless spark sound source is an impulsive electro-acoustic transducer. It generates a broadband impulse which is typically several tens of microseconds in duration. The electrodeless spark principle is described, and the results of parametric studies presented. It is found that the device is long lived, its emitted pressure waveform can be readily controlled, the emitted waveform is extremely reproducible, and the bubble pulse emission can be virtually eliminated.

The peak pressure developed at one yard is typically a few tenths of a bar to several bars. The electro-acoustic efficiency is modest, usually being no more than a few percent.

A discussion of several specific device configurations shows that the waveform of the emitted pressure is strongly dependent upon both the electric and, particularly, the geometric parameters used.

-ii-

CONTENTS

ILLUSTRATIONS

I. INTRODUCTION

For several years ONR, code 468, has supported research at Avco on the electrode-less spark sound source. Our research has encompassed a fairly broad range of topics. It was concerned initially with the physics of the electrodeless spark discharge and, more recently, with allied problems in broadband underwater acoustics.

In the course of our research we have found that the electrodeless spark device has a number of characteristics which are unique; characteristics which make the device particularly useful as a research tool. The following report is a summary of these findings, emphasizing those parametric, configurational, and operating considerations which most affect the acoustic characteristics of the device.

It is imprecise to refer to _the_ electrodeless spark device, since there has evolved a whole spectrum of devices, each having characteristics appropriate to a particular application or category of application. The devices vary in size, source level, directivity, pulse duration, etc. and require various electrical configurations for operation. However, the following characteristics are common to all regimes of operation and may be considered representative of electrodeless spark discharges:

1. Excellent reproducibility of waveform, shot-to-shot and day-to-day

2. Essentially no ignition time jitter (less than 10 nanoseconds)

3. Considerable control of emitted waveshape (and frequency content by implication).

4. A capability for suppression of the bubble pulse emission.

-1-

A.   THE ELECTRODELESS SPARK PRINCIPLE

The electrodeless spark is an underwater electroacoustic transducer which con-
verts capacitively stored electrical energy into broadband underwater acoustic
impulses. Figure 1 diagrammatically illustrates the electrodeless spark device.
It is superficially similar to a conventional underwater spark source; however,
the presence of the pierced dielectric barrier between the two conductors con-
siderably alters the character of the discharge.

Electrodeless spark acoustic impulses are generated by the following sequence of
events. When the switch is closed, current flows between the two submerged con-
ductors. Because a pierced dielectric barrier is interposed between the con-
ductors, the current is constrained to flow through a small aperture in the
dielectric. High electrical gradients in the aperture result in dielectric
breakdown of the electrolyte, and creation of a spark. Electrical energy from
the capacitor is dissipated in the spark, heating it, resulting in a rapid ex-
pansion of the spark, and an acoustic impulse.

B.   ACOUSTIC CHARACTERISTICS OF THE ELECTRODELESS SPARK DISCHARGE

   1.   General Characteristics

   The electrodeless spark device emits an acoustic waveform consisting of an
   intense, short duration, condensation pulse; a prolonged, low amplitude
   rarefaction, or "tail"; and one or more low amplitude bubble pulses. The
   time history of the emitted pressure is diagramatically illustrated in
   Figure 2.

   The peak level, shape, and duration of the initial condensation pulse depends
   upon the electrical and geometrical parameters employed. Similarly the in-
   tensity and duration of the rarefaction depends principally upon the energy
   of the discharge and the static pressure (or developed pressure if the dis-
   charge is confined by a housing).

   The bubble pulse emission is very short duration (several microseconds).
   Its peak intensity depends upon the effectiveness with which it is sup-
   pressed. If no bubble pulse suppression is used, the first bubble pulse
   may have a peak level which is several times more intense than the peak level
   of the primary condensation. On the other hand, bubble pulse suppression
   techniques have been developed which can reduce the emission so that its peak
   level is very low relative to the peak level of the primary condensation
   pulse. The factors involved in these techniques will be discussed in detail
   in a later section.

   As mentioned above, the peak levels, pulse duration, device size, etc. vary
   considerably depending upon the configuration used. Table I is a summary of
   representative acoustic characteristics which have been observed. Two devices
   with their electrical and geometric configurations will be discussed in detail.
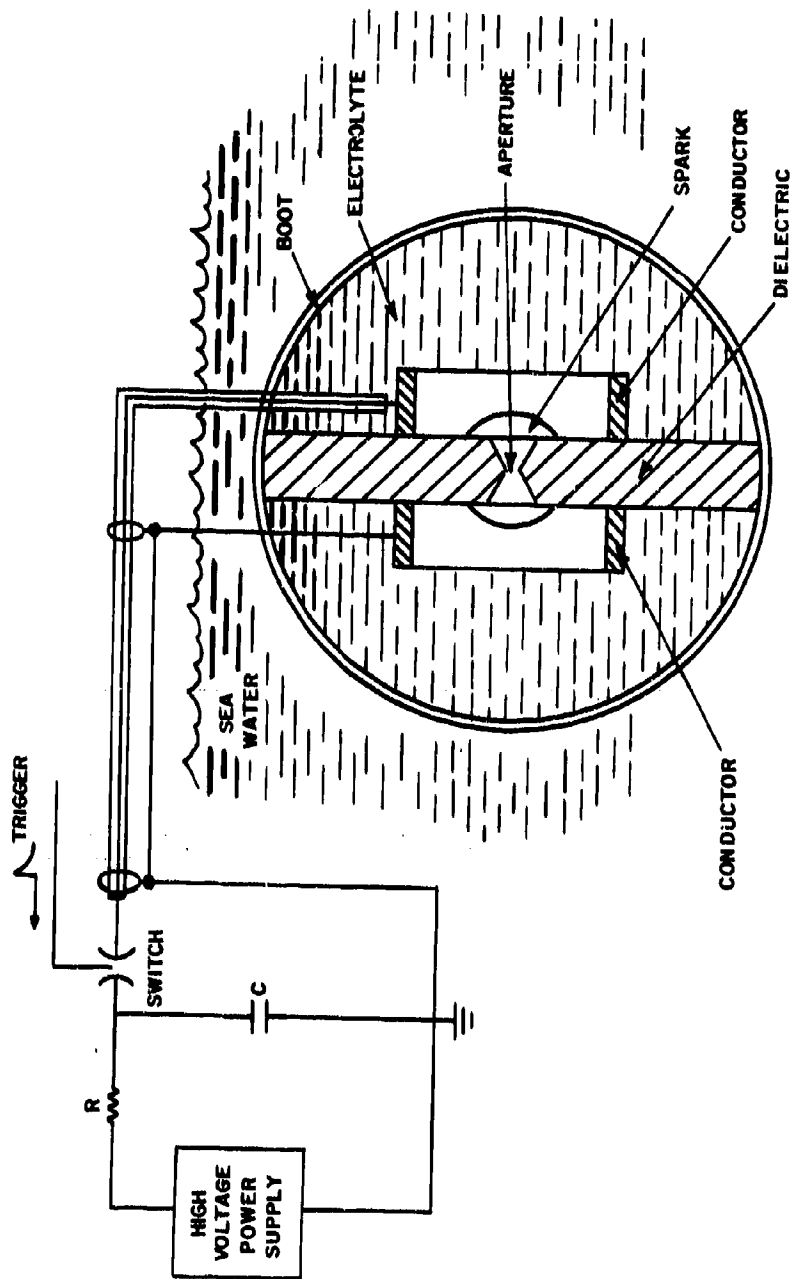
Figure 1 THE ELECTRODELESS SPARK DEVICE

ELECTROLYTE

APERTURE

SPARK

CONDUCTOR

DIELECTRIC

BOOT

CONDUCTOR

TRIGGER

SEA WATER

SWITCH

C

R

HIGH VOLTAGE POWER SUPPLY

89-5688
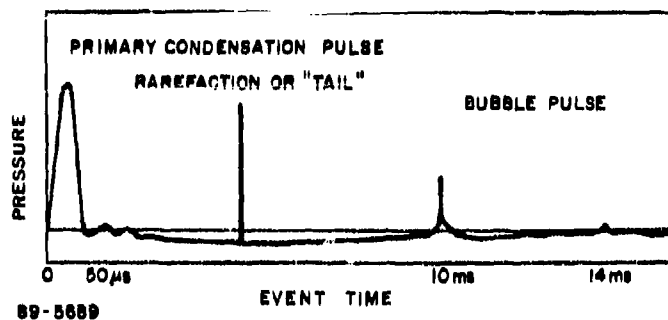
Figure 2 REPRESENTATIVE ELECTRODELESS SPARK PRESSURE WAVEFORM

TABLE I

Stored Elec. Energy (joules)	Capacitance (μf)	Voltage (kv)	Capacitor Size (in.^{3})	Device Size (in.^{3})	Pulse Length (μs)	Peak Pressure @ 1 yd. (dB re μb)
30	0.1	24.5	42	10	1.5	118
100	0.5	20.0	190 42*	15	10.0	120
1,350	3.0	30.0	1,080 450*	100	40.0	133
2,700	6.0	30.0	2,160 900*	100	40.0	137

*High energy density capacitors.

2. A Low Energy Electrodeless Spark Device

The low energy electrodeless spark device generates a short condensation or impulse of several microseconds total duration. It is suitable for applications where precise reproducibility of waveform and broad spectral content are desired. Construction of the device is illustrated in Figure 3. It consists of a dielectric body (nylon), an inner conductor, a dielectric tube, a pierced dielectric plug, a 2.385-inch diameter outer housing (conductor), and a plexiglas hemispherical cap. The electrolyte used is an approximately one-half saturated (1.10 gm/cm^3 @ 70°F.) solution of solar salt. Since solar salt is produced by evaporation of ocean water, our electrolyte is essentially of ocean composition, but considerably more saline than normal ocean water.

-4-
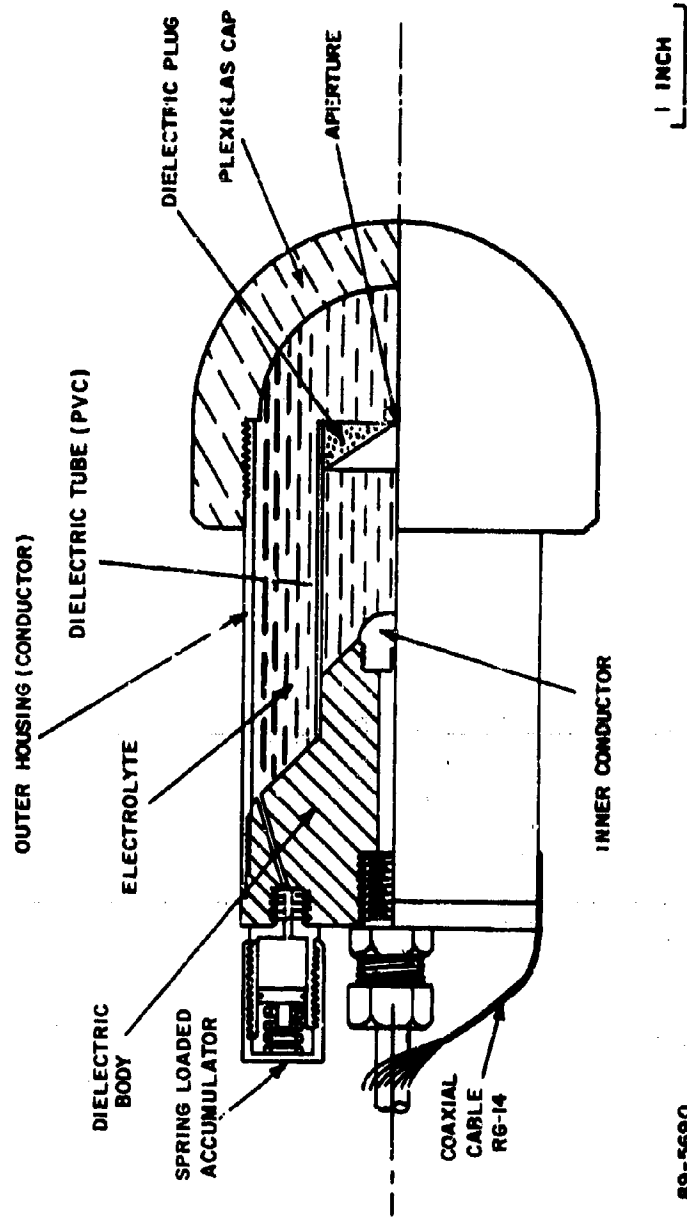
Figure 3 A LOW ENERGY ELECTRODELESS SPARK DEVICE

89-5690

-5-

The device of Figure 3 is suitable for the discharge of tens of joules of stored electrical energy. Energy dissipated per discharge is limited by the plexiglas cap. The acoustic output depends upon the electric and geometric parameters used. Condensation impulses with a total duration between two- and twenty-microseconds can be readily generated. The factors which determine pulse length and shape will be discussed in a later section.

Figure 4 is a record of the pressure observed on axis, one foot from the device, using an Atlantic Research LC-6 hydrophone. This pressure waveform can be considered representative of the acoustic emissions from the low energy device. The discharge of Figure 4 required 25 joules (20 kilovolts 0.125 microfarad) of stored electrical energy. The exponential impulse has a total duration to the first baseline crossing of approximately twelve microseconds. The peak pressure generated in this instance was 110 dB above one dyne/cm^2 at one yard equivalent.

89-5691
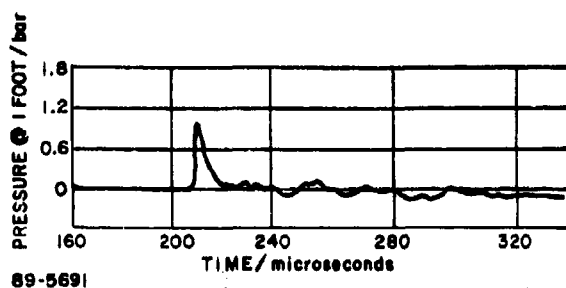
Figure 4 PRESSURE OBSERVED ONE FOOT FROM A 25-JOULE
ELECTRODELESS SPARK DISCHARGE

The spark created by the electrodeless discharge is physically small. It is almost spherically symmetric and expands radially. As a result, the electrodeless spark device is essentially omnidirectional, except for what might be called structural effects, e.g., refraction by the cap, diffraction around the edge of the aperture plug, reflection from the outer housing, masking by the body, etc. Because the low energy source is cylindrically symmetric, and because there is very little masking of the spark in the forward hemisphere, the device of Figure 3 is almost omnidirectional in the front hemisphere. Figure 5 is the broadband directivity pattern at one yard in the X Y plane, where the acoustic (geometric) axis has been designated the + X coordinate. It is virtually omnidirectional in the YZ plane.

3. A High Energy Electrodeless Spark Device

The electrodeless spark device which is illustrated in Figure 6 is representative of devices suitable for the dissipation of several kilojoules of stored electrical energy. It consists of a dielectric body (epoxy fiberglas in this case), two circular ring conductors, and two compliant dielectric boots. The electrolyte used in this device is also a 1.10 gm/cm^3 solution of solar salt. Coaxial RG-14U cable is used to connect the source to its energy storage capacitor.

-6-

Figure 5 BROADBAND DIRECTIVITY PATTERN OF A LOW ENERGY
ELECTRODELESS SPARK

89-5692

-7-

BOOT CUT AWAY
TO SHOW APERTURE

A — A

HYDRODYNAMIC SCREEN
APERTURE
BOOT
ELECTROLYTE
DIELECTRIC BLOCK

SECTION "AA"

89-5693

Figure 6 A DOUBLE-BOOTED ELECTRODELESS SPARK DEVICE

-8-

An acoustic pressure which is representative of the emission from this de-
vice is shown in Figure 7. It is a smoothly rounded pulse resembling one-
half cycle of a sinusoid, which is approximately 50 microseconds in total
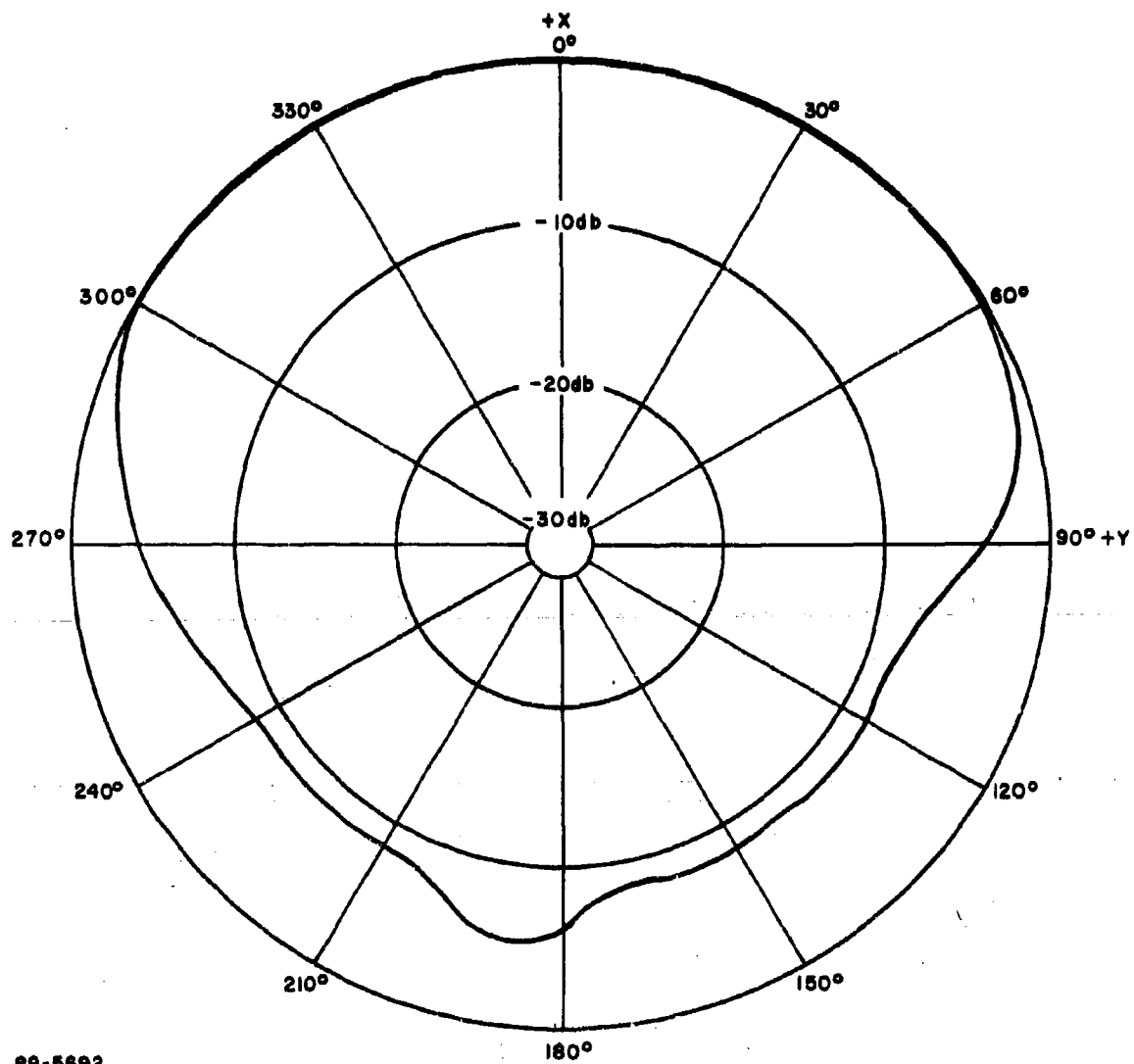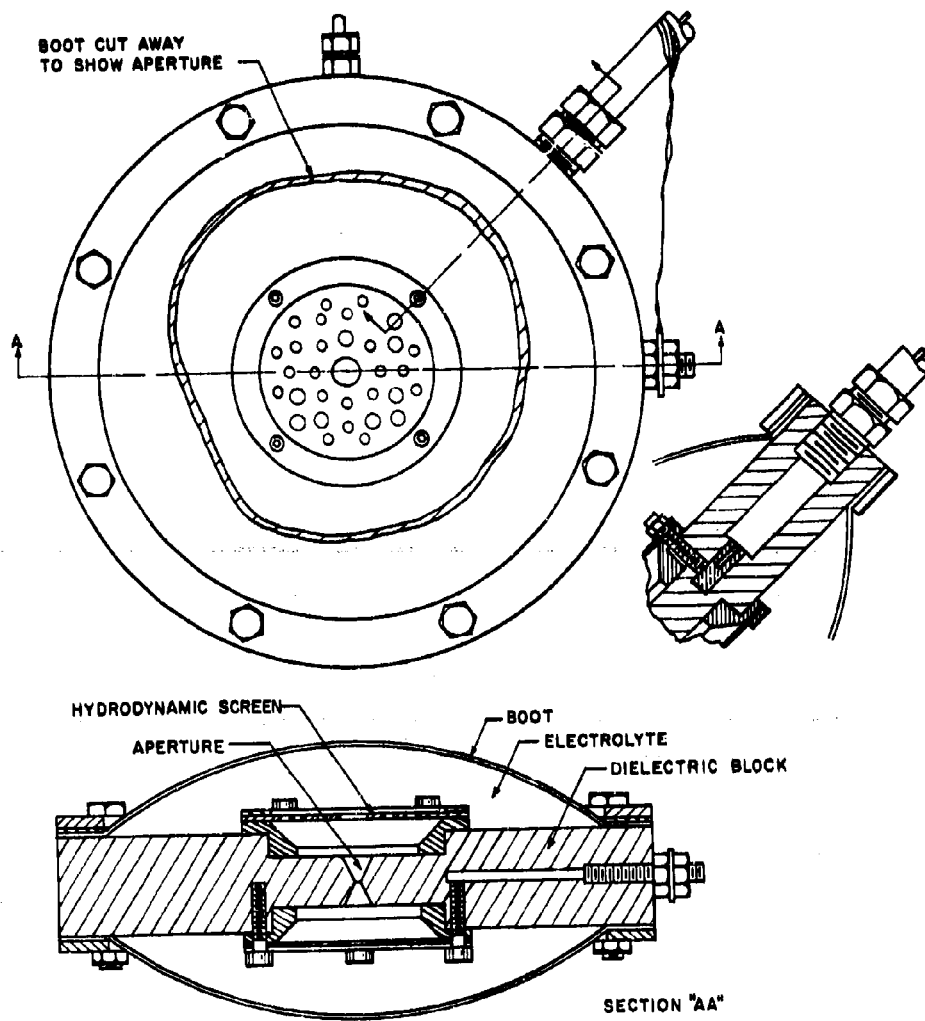duration. The pulse shown in Figure 7 has a peak pressure at one yard
which is about 128 dB above one dyne/cm^2.

This double-booted device is very nondirective. Its XY-plane beam pattern
is shown in Figure 8, where the + X axis has been chosen normal to the plane
of the device body. Because of symmetry, the device is essentially omnidirec-
tional in the YZ plane.

C. ACOUSTIC ENERGY SPECTRAL DENSITY

If an acoustic source is cyclic, in the sense that it returns after an event to
its original configuration, then the time integral of the emitted pressure must
be negligible. This is the case with the electrodeless spark source; however,
the pressure emitted by the electrodeless device is not symmetric in time, i.e.,
it consists of a short duration, intense, condensation pulse followed by a long
duration, low amplitude, rarefaction, or "tail". The condensation pulse is
generated by the radial acceleration of the spark due to dissipation of elec-
trical energy. The rarefaction, or "tail", is a result of deceleration and
collapse of the spherical void generated by the spark.

Page[1] has shown that the energy spectrum of a "signal", can be considered time
dependent. This fact is particularly significant when considering the acoustic
spectral density of a pressure waveform such as that emitted by the electrodeless
device. The initial condensation pulse may for some purposes be virtually separ-
able from the rarefaction, as for example, in laboratory scattering studies. As
a result, it is useful to consider the acoustic energy spectral density of the
condensation pulse emitted by the electrodeless device both with, and without,
its "tail", or rarefaction portion.

Because of instrumental limitations and tank reverberation, it is not possible
at Avco to experimentally measure the spectral density of either the condensation
or rarefaction pulses. However, the spectral density has been estimated using an
analytical approximation to the observed and deduced pressure waveforms.

The pressure emitted by the electrodeless device consists of a pulse which we
have represented by one-half cycle of a sinusoid, and a rarefaction which is of
considerably longer duration, also represented by one-half cycle of a sinusoid.
Let the emitted pressure, p(T) , be given by

$$p(T) = \begin{cases} \dfrac{A}{r} \sin a T & 0 < T < \pi/a \\[2em] \dfrac{B}{r} \sin b(T - \pi/a) & \pi/a < T < \pi/b \\[2em] 0 & \text{otherwise} \end{cases} \qquad (1)$$
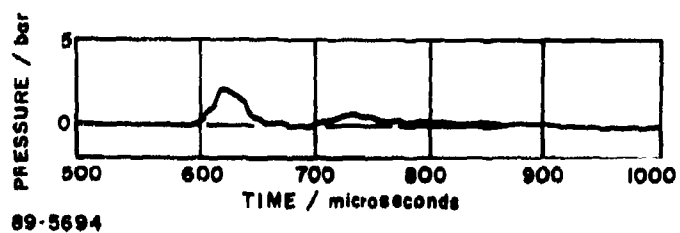
-9-

Figure 7 PRESSURE OBSERVED ONE YARD FROM A 3,200-JOULE DISCHARGE
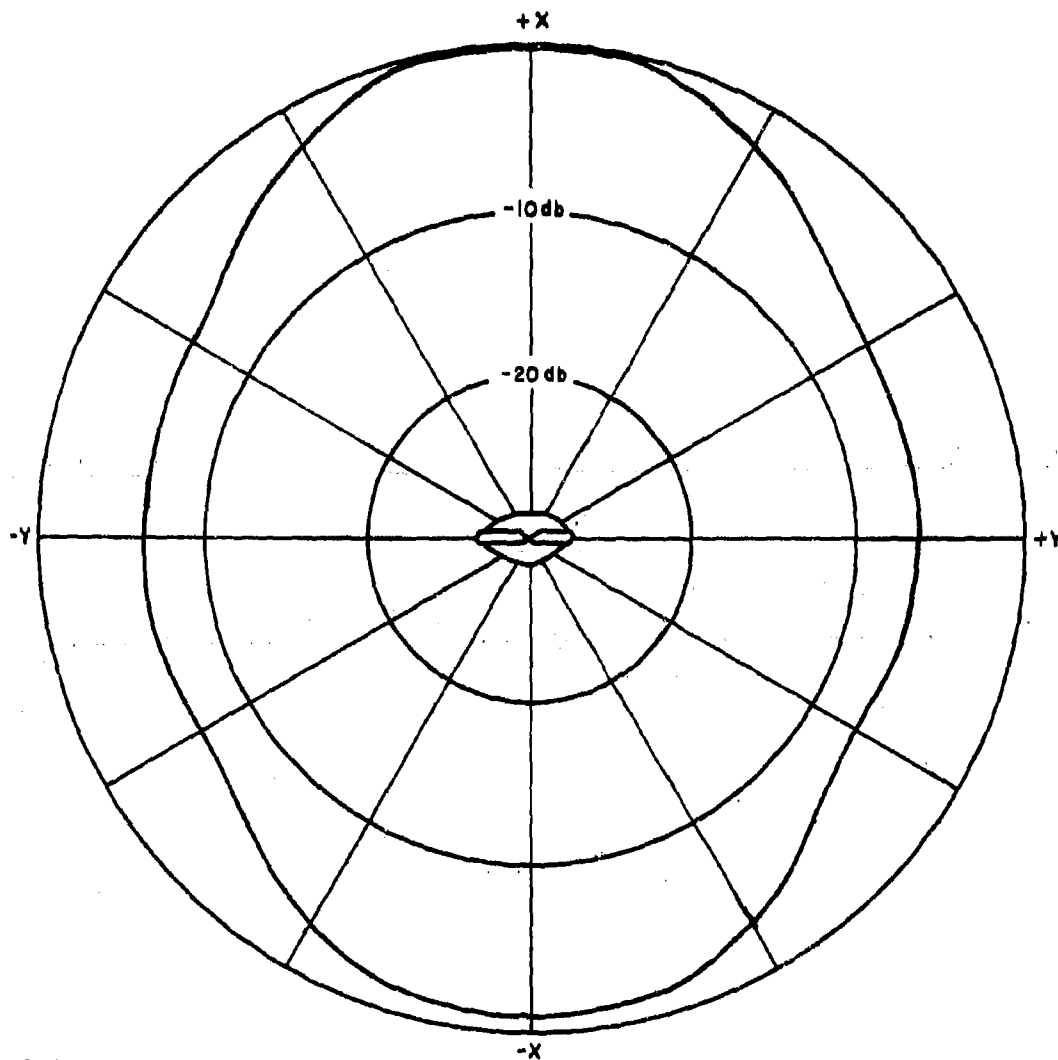
89-5694

89-5695

Figure 8 BROADBAND DIRECTIVITY PATTERN OF A DOUBLE-BOOTED
ELECTRODELESS SPARK DEVICE

where t is time, r is distance from the source, c is the velocity of sound, A and B are the magnitudes of the pressures at a reference distance, a and b are reciprocal time parameters, and $T = t - r/c$ is a delayed time.

The acoustic energy of the condensation pulse, E_c, is given by

$$E_c = 2 \pi r^2 (\pi A^2 / \rho c a) \tag{2}$$

and that of the rarefaction pulse, E_r, by

$$E_r = 2 \pi r^2 (\pi B^2 / \rho c b). \tag{3}$$

The time integral of the pressure is zero provided

$$B = bA/a. \tag{4}$$

Dividing (3) by (2) and applying (4) we find that the ratio of acoustic energy represented by the rarefaction pulse to the energy of the condensation pulse is given by the ratio b/a. We have concluded that if our waveform is very asymmetric in time, so that $b/a \ll 1$, then virtually all the radiated energy resides in the intense condensation pulse. This result is consistent with the analysis of Junger[2], which showed that, if a fluid is rapidly accelerated, then gradually decelerated; one-half of the energy imparted to the fluid will be radiated to the far field as an acoustic condensation pulse, whereas only a small portion of the remaining energy will be radiated to the far field in the form of a rarefaction pulse.

The double-booted, high energy electrodeless spark device generates a condensation pulse of about 50 microseconds duration and a rarefaction pulse of about 10 milliseconds duration. Using these parameters in the waveform of Equation (1), we find that the acoustic energy spectral density is as shown in Figure 9. The scale of the abscissa has been greatly expanded in the lower curve. It can be seen that even though the rarefaction pulse represents only a small portion of the total emitted energy, its effect upon the very low frequency portion of the spectrum is pronounced. The spectral density below about 150 Hz is considerably altered in this case by the "tail".

The mechanics involved in the low energy electrodeless spark discharge are somewhat different from those of the double-booted device. The semi-rigid housing of the low energy device constitutes a constraint which results in a transient rise in internal pressure following each discharge. As a result, the inertially expanding void created by the discharge is decelerated more rapidly than would have been the case had there not been the constraint of the device housing. Since deceleration of the spark void is associated with the rarefaction pulse, or "tail", the duration of the rarefaction is shortened, being typically about 300 microseconds in duration. It was seen that a representative condensation pulse was about ten microseconds in total duration. Combining these parameters, as above, we find that the spectral density can be estimated as shown in Figure 10. The lower record has a greatly expanded abscissa to show the effects of the rarefaction pulse upon the low frequency portion of the spectrum. It can been seen that the overall bandwidth is great for this short-pulse device, however, the spectral density of the entire emission, pulse plus rarefaction, is not rich in low frequency energy. The condensation pulse, considered separately, is rich in low frequency energy.

-11-
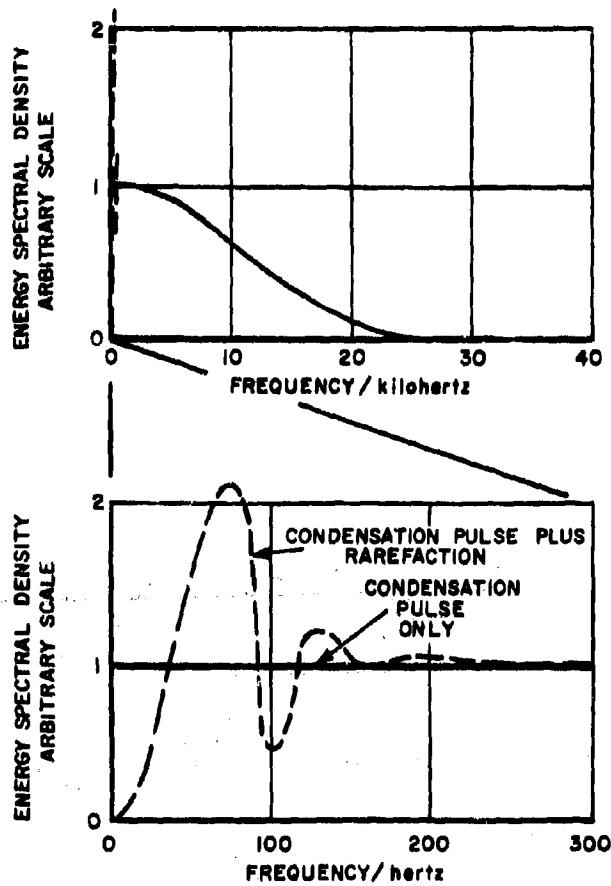
89-5696

Figure 9 THE CALCULATED ACOUSTIC SPECTRAL DENSITY OF 50-MICROSECOND
CONDENSATION PULSE BOTH WITH AND WITHOUT A
10-MILLISECOND RAREFACTION
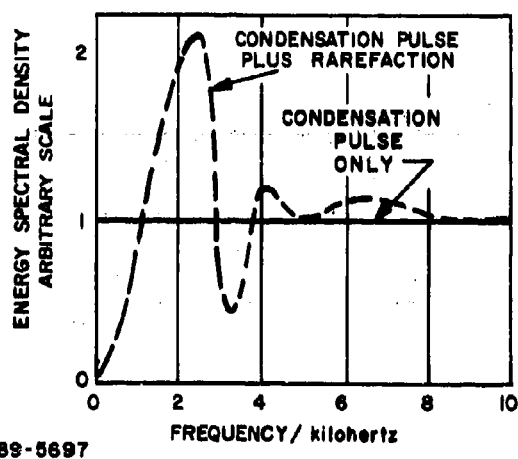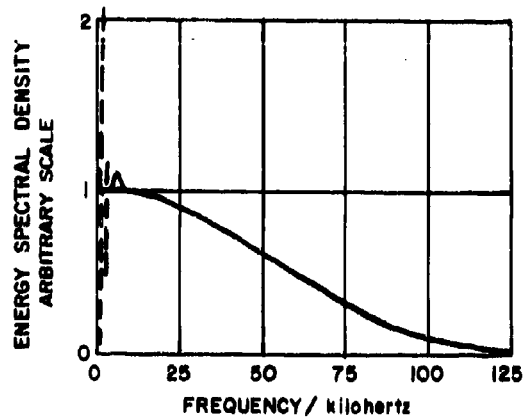
Figure 10 THE CALCULATED ACOUSTIC SPECTRAL DENSITY OF THE PRESSURE
EMITTED BY A LOW ENERGY ELECTRODELESS SPARK SOURCE

89-5697

-13-

The spectral densities shown in Figures 9 and 10 should be considered representative only, since modifications are readily achievable which will considerably change the emitted acoustic spectral density. For example, variations of aperture geometry will modify the pulse duration, so as to result in perhaps a five- or twenty-microsecond pulse rather than the ten-microsecond pulse used in the calculation. Changes of this sort will clearly affect the emitted acoustic spectrum considerably.

D. DISCHARGE MECHANICS AND WAVEFORM CONTROL

The electro-mechanical processes involved in the electrodeless spark discharge are similar to those of a conventional underwater spark discharge; however, there are important electrical and mechanical effects which result from the presence of the dielectric block in which the discharge takes place. Because of complexities involved in quantitative analysis of the discharge physics, we have found that the most meaningful progress has resulted from experimental effort, i.e., parametric studies and qualitative theoretical considerations. By far the most important "parameter" in the electrodeless spark device is the shape of the aperture. Aperture geometry affects both the shape of the acoustic pulse and the efficiency of the discharge. The two effects will be discussed in the following.

1. Waveform Control

As discussed previously, the electrodeless spark device consists of a "sandwich" composed of a metallic conductor, electrolyte, a pierced dielectric block, electrolyte, and a second conductor. Electrolytic current is constrained to flow through the aperture in the dielectric block. Because the diameter of the aperture is small, the current density and voltage gradients in the aperture are great, and spark breakdown occurs in the aperture.

There are several results of the fact that the spark develops in the aperture. Perhaps the most important is that the control can be exercised over the emitted waveform. Waveform control stems from the fact that the spark is in series with the electrolyte. Since the time history of the resistance of the electrolyte is determined by the aperture shape, it follows that aperture shape also determines the time history of the spark discharge. For example a wide-angle aperture configuration, such as illustrated in Figure 11 results in a minimal electrolytic resistance and a short duration event. On the other hand, a long narrow aperture, such as illustrated in Figure 12 results in considerable electrolytic resistance in series with the nascent spark, so that development of the spark is slowed and the duration of the discharge extended. As a result, the acoustic emission tends to develop slowly and to be of relatively prolonged duration.

It will be seen in the next section that aperture geometry affects the efficiency of the discharge. It will be shown, as well, that electrical parameters, particularly capacitance and initial voltage, also affect both the efficiency of the discharge and the acoustic waveshape. The optimum aperture geometry and electrical parameters tend to be determined by the particular application. Specific examples are perhaps useful.

-14-
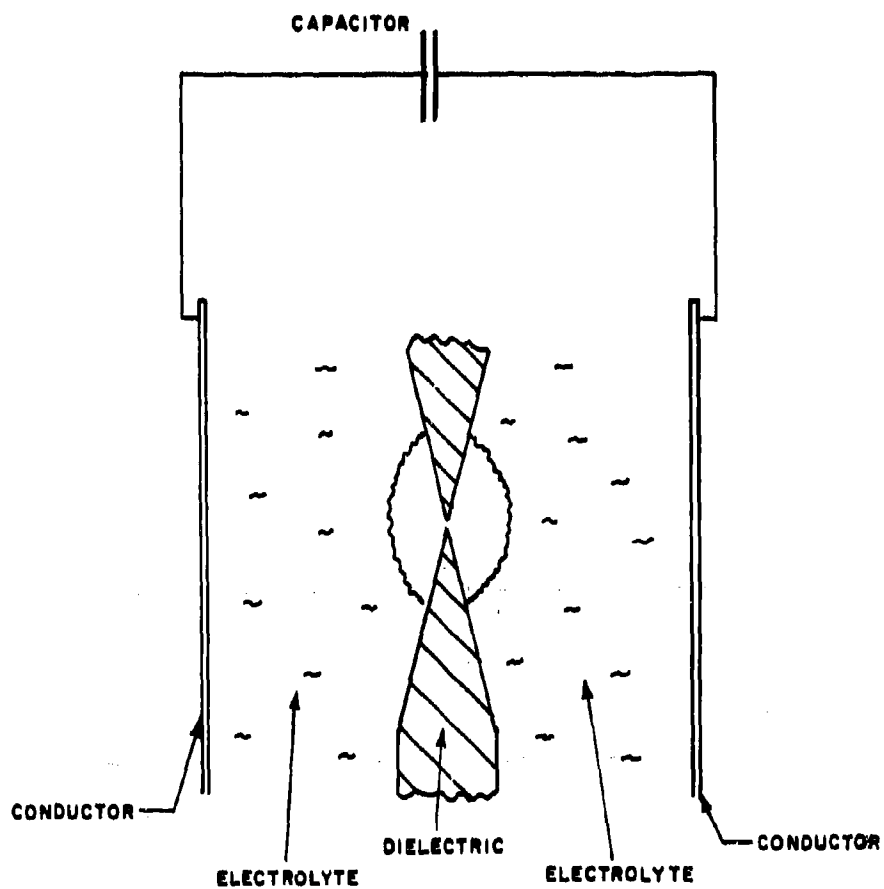
Figure 11 A WIDE ANGLE APERTURE CONFIGURATION

89-5698

CAPACITOR

CONDUCTOR   ELECTROLYTE   ELECTROLYTE   CONDUCTOR
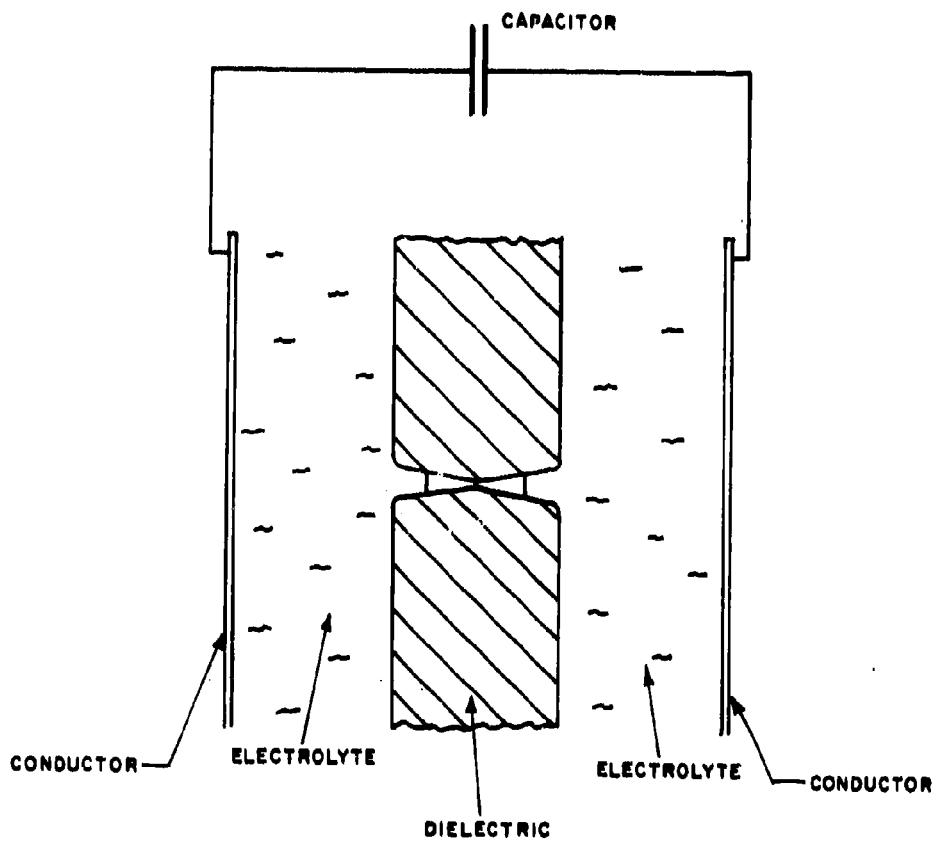
DIELECTRIC

89-5699

Figure 12 A NARROW APERTURE CONFIGURATION

-16-

The short length, wide angle aperture illustrated in Figure 13 is suitable for the discharge of tens of joules of electrical energy. The 25-joule discharge cited as an example involved the use of 0.125 microfarad capacitance and 20 kilovolts. The pressure was recorded using an Atlantic Research LC-5 hydrophone at twelve inches. Allowing for the apparent hydrophone resonance, it can be seen that the pressure emitted by this combination of parameters was an exponentially decaying pulse of approximately ten microseconds duration. Because the aperture is rather wide angle, and the capacitance only modest, the initial rate of pressure increase was great and the duration of the pulse short.

Figure 14 illustrates a second case. In this second example the aperture is about twice as long as in the first example and the electrical capacitance is greater. The spark was initiated in the center of the aperture so it was initially in series with greater electrolytic resistance. The result was that the spark developed more slowly. The additional capacitance was sufficient to sustain the discharge for a longer period. The emitted pulse duration was approximately twenty microseconds and the waveshape nearly sinusoidal.

A third example is illustrated in Figure 15. In this instance an approximately fifty microsecond pulse was generated by the discharge of eight microfarads charge initially to 28.3 kilovolts. Once again the initial resistance of the device was fairly large, so that the spark development was gradual. The pressure pulse is nearly sinusoidal in shape.

2. The Effects of Aperture Geometry Upon Efficiency

In the case of the electrodeless spark the resistance of the electrolyte is an important factor in determining the electro-acoustic efficiency of the discharge. Designating the electrical resistances of the spark and the electrolyte by R_s and R_w respectively, we find that since the two are in electrical series, the power dissipated in the spark, P_s, is given by

$$P_s = E^2 R_s /(R_s + R_w)^2 \tag{5}$$

where E is the capacitor voltage.

When the electrodeless spark is first struck it is in series with the electrolyte of the aperture throat. Referring to Figure 16, the magnitude of the electrolytic resistance of the throat is given by

$$R_w = (\ln L - \ln r_s) / \pi \sigma (1 - \cos \theta) \tag{6}$$

where σ is the specific conductivity of the electrolyte, θ is the half angle of the throat, r_s is the radius of the spark, and L is the aperture length.

0.050

20 kilovolts

60°

- 0.125 microfarad

0.020
DIA.

25 joules
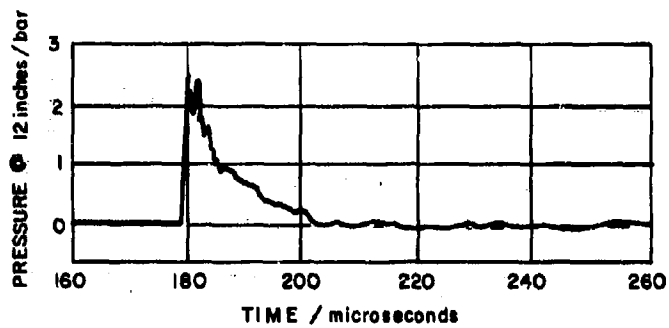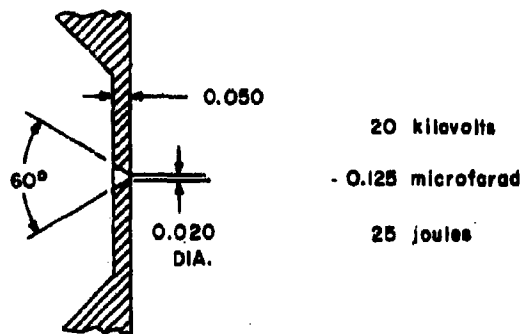
89-5700

Figure 13 ELECTRICAL, CONFIGURATIONAL, AND ACOUSTICAL CHARACTERISTICS
OF A LOW ENERGY ELECTRODELESS SPARK DISCHARGE

-18-

0.110

55°

0.020
DIA.

IC kilovolts

I microfarad

50 joules
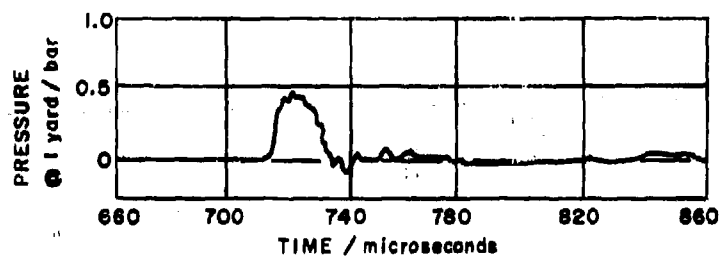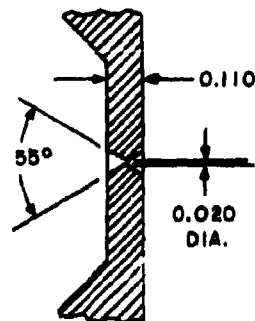
89-5702

Figure 14 ELECTRICAL, CONFIGURATIONAL, AND ACOUSTICAL CHARACTERISTICS
OF AN ELECTRODELESS SPARK DISCHARGE

-19-

28.3 kilovolts

8.0 microfarads

3,200 joules
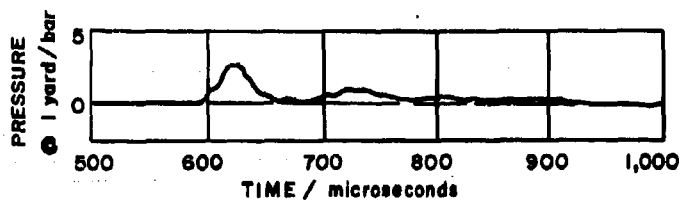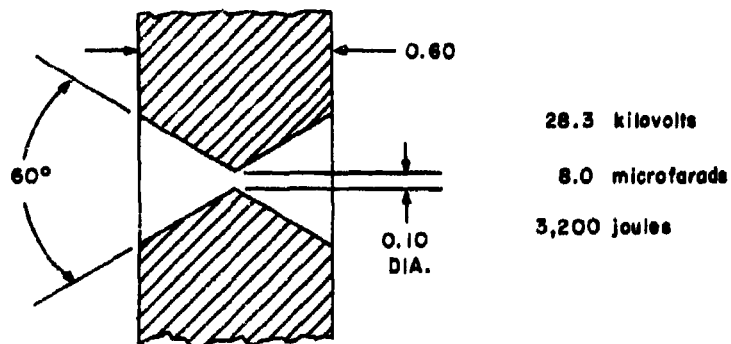
Figure 15 ELECTRICAL, CONFIGURATIONAL, AND ACOUSTICAL CHARACTERISTICS
OF A HIGH ENERGY ELECTRODELESS SPARK DISCHARGE
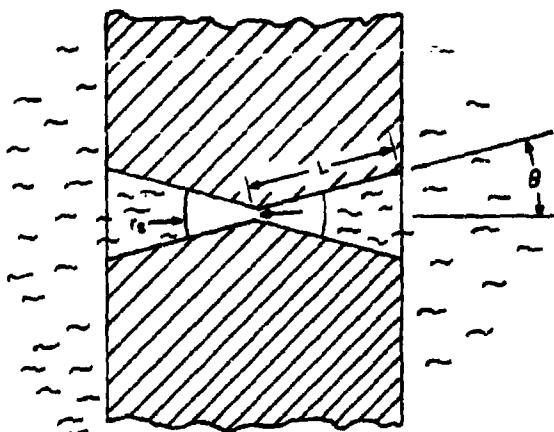
89-5704

89-5705

Figure 16 COORDINATES USED IN DISCUSSION OF EFFICIENCY

Even if a wide angle aperture is used the resistance of the electrolyte will be large initially. For example, if the radius of the nascent spark is one millimeter, the electrolytic resistance of highly saline salt water will initially be tens of ohms. Caulfield[3] has found that the electrical resistance of an intense underwater spark is about one ohm. Comparable spark resistance can be expected for the electrodeless spark. It follows that the electrical power will, at first, be dissipated mostly in the electrolyte. Only after the spark has grown larger can the power dissipated in the spark be a large portion of the total power dissipation. As a result, a wide angle aperture configuration tends to result in modest efficiency, because the stored electrical energy is dissipated while the resistance of the spark is small compared to the resistance of the electrolyte.

The optimum aperture configuration, from an efficiency viewpoint, has been found to be a horn or bell-shaped aperture, as illustrated in Figure 17. If the length of the aperture is chosen so that there is a significant portion of the initial electrical energy still available on the capacitor when the spark has grown to the shoulder of the aperture, then as the spark expands past the edge, the electrolytic resistance in series with the spark drops rapidly, and the power dissipation increases greatly. Since, by this time, the electrical resistance of the electrolyte is equivalent to or smaller than the electrical resistance of the spark, a greater proportion of the electrical power is dissipated in the spark.

The length of the aperture must be compatible with the electrical parameters. If the aperture is too long, too much of the electrical energy will be dissipated in the process of developing the spark, i.e., generating a spark which fills the aperture cavity. If it is too short, too much energy will be dissipated in the electrolyte while the spark is small.

-21-
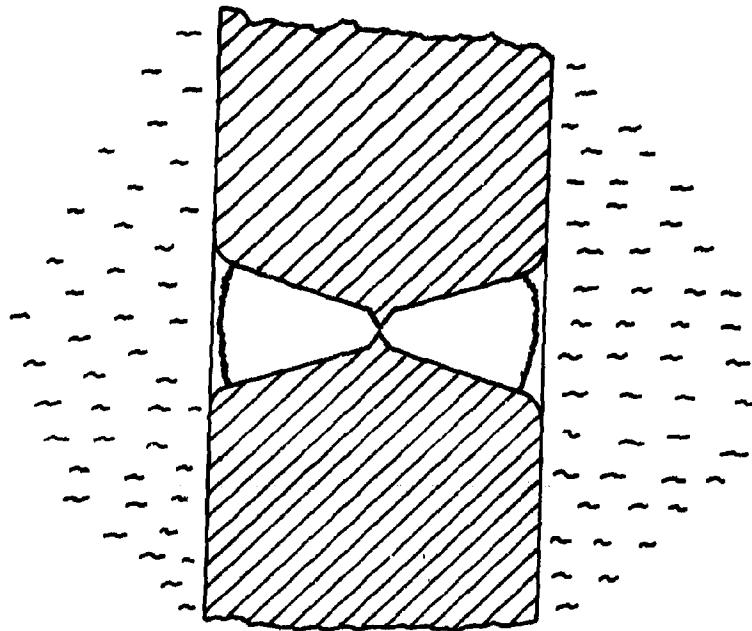
89-5706

Figure 17 A BELL-SHAPED, SHOULDERED APERTURE CONFIGURATION

We found that an aperture length of 0.30-inch (0.6-inch total dielectric thickness) is optimum when capacitances of 6- to 10-microfarads are used at voltages from 20- to 30-kilovolts. Discharges using these parameters with a shouldered, or bell-shaped aperture configuration, result in the highest electro-acoustic efficiencies (several percent).

3. Reproducibility

The pressure emitted by the electrodeless spark device is extremely reproducible; provided there is no undissolved gas present in the aperture prior to the discharge. Undissolved gas has a dielectric strength which is low compared to water. It is felt that as a result, the bubbles of gas in the aperture break down electrically when the voltage gradients rise during a discharge. The result is a multitude of randomly positioned sparks and poor reproducibility of acoustic output.

Undissolved gas can be prevented by either 1) degassing the electrolyte prior to use, 2) by applying a static pressure to force the gas into solution, or by 3) circulating the electrolyte through the aperture continuously in order to flush out bubbles.

In the case of confined devices, such as the low energy device of Figure 3, mechanical flushing of the electrolyte can be accomplished by simply connecting the outer and inner regions of the device with dielectric tubing containing a check valve and an accumulator. The transient rise in internal pressure following the discharge will compress the accumulator. As the internal pressure drops the accumulator will force its electrolyte into the inner compartment and through the aperture. The check valve assures circulation so that there is flow through the aperture. This technique has been tested and found to be feasible.

4. Optically Dense Electrolytes

Martin[4] reports temperatures of underwater sparks of 20,000° - 30,000°K. Measurements of the electrodeless spark indicate comparable temperatures. Since thermal radiation from a black body is proportional to the fourth power of temperature, the radiant emission from the discharge is very intense. We have found that by adding a water-soluble black dye to the electrolyte there can be a significant increase in the electro-acoustic efficiency. Optically dense electrolytic solutions result in reabsorption of radiant energy close to the spark, increase vaporization, and increased internal spark pressure, and as much as a three decibel increase in peak radiated farfield pressure. Thermal radiation from the spark clearly is an important aspect of the energy budget of the spark-water system.

5. Multiple Operation

Because the ignition time jitter of the electrodeless spark discharge is extremely slight (less than 10 nanoseconds), electrodeless devices can be discharged either simultaneously, to generate intense directive acoustic emissions, or in a timed sequence.

Multiple simultaneous discharges are also possible within a single device by forming more than one aperture. In this case, each aperture will result in a discharge. The time history and power consumption in the apertures will be alike; provided the electrolytic resistance between the apertures is large compared to the electrolytic resistance between an aperture and the common conductor.

E. PARAMETRIC EFFECTS

As discussed above, the characteristics of the acoustic emission from the electrodeless spark discharge are largely determined by the geometrical shape of the aperture. However, other electrical and physical factors also influence the discharge.

1. Applied Voltage

We have found that the duration of the acoustic pulse emitted by the electrodeless spark device is only weakly dependent upon the applied voltage, being determined almost entirely by aperture geometry. On the other hand, the peak pressure emitted by the device is strongly dependent upon the applied voltage. An increase in applied voltage tends to result in a more than proportionate increase in emitted peak pressure and, as a result, an increase in electro-acoustic efficiency. For example, an 18 kilovolt discharge, using a particular configuration in our low energy device, results in a 16-microsecond pulse which has a peak pressure at one yard of 0.27 bar; but a 22-kilovolt discharge, with the same device configuration, results in a 17-microsecond pulse with a peak pressure of 0.48 bar. In this instance a 22% increase in applied voltage, representing approximately 50% greater electrical energy, resulted in a 78% increase in peak pressure and an approximately 220% greater acoustic energy. The dependence of peak acoustic pressure upon initial voltage is generally as illustrated, i.e., increase in applied voltage result in increases in electro-acoustic efficiency, and usually only a slight change in pulse duration or shape.

2. Capacitance

For every device configuration there is a range of suitable or desirable capacitance. Capacitance within this range is appropriate to the aperture configuration. The use of a capacitance which is below the "suitable" range results in a considerable loss of efficiency. Increases in capacitance within the suitable range result in increases in emitted peak pressure and often modest increases in electro-acoustic efficiency. The use of a capacitance which is excessively large results in a loss of efficiency.

For example, a discharge using 0.125-microfarad capacitance and a particular configuration, results in a 16-microsecond pulse which had a peak pressure at one yard of 0.39 bar; whereas a 0.250-microfarad discharge in the same device resulted in a 17-microsecond pulse with a peak pressure of 0.59 bar. In this instance a doubling of capacitance, representing a 100% increase in electrical energy, resulted in an approximately 140% increase in acoustic energy. Further increases in capacitance resulted in only modest increases in acoustic pressure.

-24-

3. Temperature

The low energy electrodeless spark device has been immersed in a water bath and the acoustic pressure recorded at bath temperatures between 35 and 85 degrees Farenheit. We found that the acoustic output is virtually the same at all temperatures within the test range. The peak pressures observed were all within 5% of the peak pressure observed at room temperatures.

4. Static Pressure

Two tests have been made of the effects of static pressure. In the first the low energy device, shown in Figure 3, was internally pressurized to zero, 20, 40, and 60 psi above atmospheric pressure. In each instance the pressure emitted by a 25-joule discharge was recorded. We found that the peak radiated pressure increased slightly with increased internal pressure.

The pulse duration and waveform were not significantly affected otherwise. The peak radiated pressure with a 60 psi internal pressure was one dB above the peak radiated pressure with zero internal overpressure. In all cases the emitted pulse duration was approximately six microseconds.

The second test involved discharge of the low energy device inside the chamber of our pressure vessel. An uncalibrated, high frequency probe hydrophone was mounted nine inches from the source, on axis. Both source and hydrophone were subjected to static pressures up to 10,000 psi. The radiated pressure was recorded for both 15- and 30-joule discharges. We found that the peak pressure emitted by the discharges increased about two dB as a result of an increase of static pressure from atmospheric to 80 psi above atmospheric. Further increases in static pressure resulted in additional, very modest increases in peak radiated pressure. Discharges at 2,000 through 10,000 psi above atmospheric pressure were uniformly about 3.4 dB above the peak pressure observed at atmospheric pressure.

It was concluded that the primary condensation pulse from low energy electrodeless spark discharges are enhanced as a result of modest static pressures of 60 to 100 psi, but are relatively unaffected by additional increases of static pressure up to 10,000 psi.

It is apparent that the duration and intensity of the rarefaction following the discharge will be greatly affected by increased static pressure. Direct measurement of the duration and shape of the rarefaction pulse was not possible because of tank reverberation.

It was noted previously that the pressure waveform emitted by the electrodeless spark is extremely reproducible, provided there is no undissolved gas in the aperture prior to the discharge. It is apparent from this fact and the above discussion that the electrodeless spark device operates both most reproducibly and most efficiently when exposed to at least a modest static overpressure.

F. BUBBLE PULSE SUPPRESSION

Most impulsive underwater sound sources produce an intense bubble pulse. The bubble pulse is a result of cavitational collapse of the gaseous void created by

the impulse event. Junger[2] shows that if work is done upon a fluid impulsively, then the energy represented by the acoustic pulse radiated to the far field is only one-half of the total work done upon the fluid. The remaining energy is available in the nearfield in the form of kinetic (and later potential) energy. The cavitational collapse of the void created by an underwater discharge results in radiation to the farfield of some of this remnant energy. Hersey[5], et al. report bubble pulse peak pressures following underwater spark discharges which are several times greater than the peak pressure of the initial condensation pulse.

In some applications the bubble pulse emission constitutes a serious limitation to the utility of the source. In the following there are discussed two techniques for suppression of the bubble pulse emission. The first technique is hydromechanical and the second is electrical.

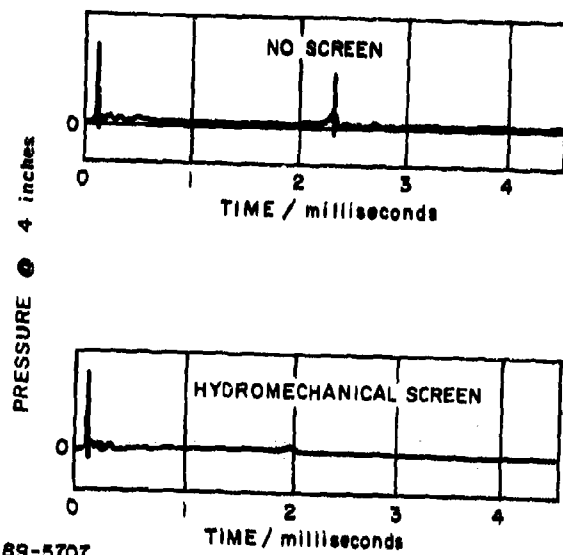### 1. Hydromechanical Bubble Pulse Suppression

The underwater electrodeless spark event creates an intense local pressure which propagates outward acoustically. The propagation of this condensation pulse requires only microscopic fluid displacements.

The impulsive electrodeless spark event also imparts to the water a radial velocity which persists, because of the inertia of the water, causing the cavity formed by the event to increase in size. This outward flow of water is decelerated by the hydrostatic pressure, eventually stopped, and inward flow begun. The inward flowing water compresses the gas contained in the cavity, eventually producing a small, high pressure bubble and reversal of the direction of flow. It is the "bottoming out" of the walls of the cavity and the rapid outward radial acceleration which results in the "bubble pulse".

It is the kinetic energy of the radially flowing water which is the source of energy for the bubble pulse. Accordingly, the intensity of the bubble pulse emission can be greatly diminished if the kinetic energy of the radial flow is dissipated prior to generation of the bubble pulse. This can be accomplished by introducing a screen, or baffle, which impedes the radial flow of water. Construction of the screen may be such as to offer negligible impedance to the microscopic displacements necessary for propagation of the initial acoustic condensation pulse, but considerable impedance to the macroscopic hydrodynamic flow involved in generation of a bubble pulse.

In such a case the initial pulse will be virtually unaffected; whereas the velocity of radial flow will be diminished, so that only a weak or negligible bubble pulse will be generated.

The concept of a hydromechanical technique for bubble pulse suppression has been tested and found very effective. A test screen was fabricated using a 0.031-inch thick two-inch diameter fiberglas disk which was perforated with thirty-two, approximately 0.1-inch diameter holes. The screen was mounted approximately 0.125-inch in front of the aperture of the low energy electrodeless spark device. Since the screen was very thin it did not materially affect the condensation pulse emitted by the electrodeless spark discharge. On the other hand, the macroscopic flow following the spark discharge was significantly attenuated by the hydrodynamic impedance of the screen. Figure 18

-26-

Figure 18 DATA ILLUSTRATING BUBBLE SUPPRESSION BY A
HYDROMECHANICAL SCREEN

89-5707

illustrates the results. The upper trace is a record of the pressure emitted by a 30-joule electrodeless spark discharge. The initial condensation pulse can be seen at 0.05-millisecond and a prominent bubble pulse at 2.3-milliseconds. The lower trace is a record of the pressure observed under precisely the same electrical and configurational conditions, except that a bubble pulse suppression screen has been mounted in front of the aperture. The initial condensation pulse is still evident at 0.05-millisecond; however, the bubble pulse intensity is greatly reduced.

We have concluded that a screen, or screen-like obstruction (e.g. rods) can result in effective dissipation of the nearfield kinetic energy and, as a result, virtual elimination of the bubble pulse emission. Moreover, since there may be erosion associated with cavitational collapse, the use of a hydromechanical screen can also reduce erosion.

2. Electrical Bubble Pulse Suppression

The hydromechanical screen discussed above results in dissipation of the nearfield kinetic energy and, as a result, reduction of the intensity of the bubble pulse emission. An alternative technique is to modify the dynamics of the cavitational collapse so as to retain the energy in the nearfield where it will be gradually dissipated. The principle involved is the following:

Junger[2] showed that following an underwater discharge the remnant nearfield energy is radiated to the farfield only if there are abrupt changes in velocity i.e. by rapid acceleration or deceleration of the fluid. Since the deceleration associated with the terminal phase of the collapse can be reduced, i.e. if the inrushing chamber walls can be decelerated more gradually than would be the case in a "normal" cavitational collapse. One way to accomplish this more gradual deceleration would be to dissipate energy in the spherical chamber prior to the terminal instant, so as to initiate the deceleration sooner than would have been the case otherwise, thereby extending the period of deceleration.

Effectiveness of the technique clearly depends upon the appropriate and timely dissipation of energy in the bubble chamber. In the case of the electrodeless spark device this can be accomplished fairly readily. The gaseous bubble generated by the electrodeless spark discharge is in electrical series with the energy storage bank. It is a characteristic of the electrodeless spark discharge that there tends to be a remnant voltage on the energy storage capacitors following a discharge. This remnant voltage is typically 5-10% of the initial voltage. During the period of bubble growth and the initial stage of cavitation collapse, the ionization of the bubble is low, and its electrical resistance high; so the remnant voltage tends to persist. In the late stages of the cavitational collapse the internal temperature and electrical gradients begin to rise, so that the conductivity of the gaseous bubble increases. The result is that the remnant energy is dissipated in the collapsing chamber during the late stage of the collapse; precisely as desired for electrical bubble pulse suppression. The result is that the cavitational collapse is more gradually decelerated than would otherwise have been the case, and the bubble pulse emission is not intense.

Electrical suppression of the electrodeless spark bubble pulse has been observed experimentally. The top trace of Figure 19 is a record of the voltage on the energy storage capacitor following a 1,200-joule discharge. There is a remnant voltage of approximately 1,500 volts.

At approximately 6.4 milliseconds the ionization in the collapsing bubble increases and the remnant energy is dissipated in the collapsing bubble. The lower trace is a record of the pressure observed at one yard after the same discharge. The initial condensation pulse is apparent at 0.6 millisecond. There is a weak bubble pulse at about 8.0 milliseconds. Allowing for the 0.6-millisecond acoustic travel time to the receiving hydrophone, we find that the remnant electrical energy was dissipated beginning approximately one millisecond before the terminal instant, i.e. during the late stage of cavitational collapse. Other discharges, using different parameters for which the infusion of electrical energy was less appropriate, resulted in bubble pulse emissions which had peak pressures which were equivalent to or exceeded the initial condensation peak pressure.

In general, electrical bubble pulse suppression has been found to be far more "temperamental" than the hydromechanical technique. Fairly subtle variations in geometric or physical conditions can result in either inappropriately timed or negligibly small electrical dissipation. Our conclusion is that the concept of bubble pulse suppression by the infusion of energy late in the cavitational collapse is sound; however, practical realization of the concept is not always straightforward.

Alternative techniques for infusion of the energy, such as the use of an independent source of electrical energy which can be appropriately triggered during the cavitational collapse might prove more reliable.
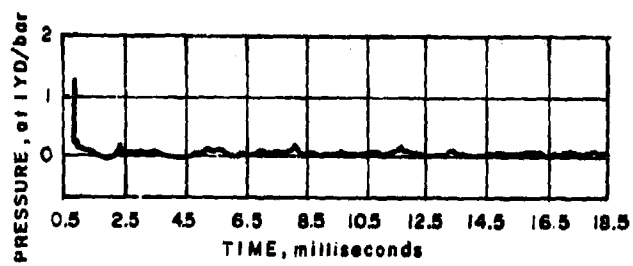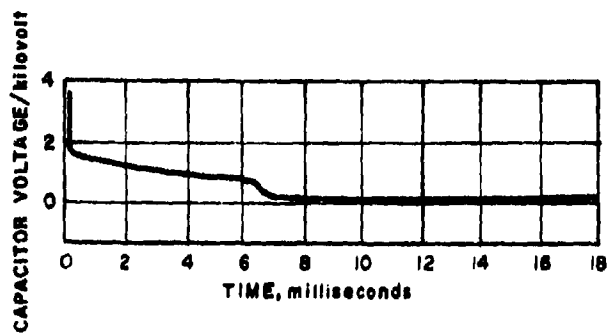
89-5708

Figure 19 DATA ILLUSTRATING ELECTRICAL BUBBLE PULSE SUPPRESSION

-30-

III. CONCLUSIONS

We have found the electrodeless spark device has the following characteristics:

1. Excellent reproducibility, shot-to-shot, and day-to-day.

2. Good control of waveform, both shape and duration.

3. Long Life.

4. A capability for the parallel operation of practically an unlimited number of devices.

5. Virtually no bubble pulse.

6. A modest electro-acoustic efficiency (up to about 3 percent).

There are several applications for which the electrodeless spark device would seem ideally suited. Because of its reproducibility and waveshape control, it is a valuable acoustic research tool. We have found it particularly well suited to experiments in broadband refraction, scattering, propagation, etc.

Because large numbers of devices can be operated in unison or in a programmed sequence, there is also a potential for the generation of both very intense and very directive broadband emissions.

The capacity for the elimination of the bubble pulse is useful in those applications in which it cannot be eliminated by time gating.

In summary, if the design and operating considerations discussed in the text are observed, the electrodeless spark underwater sound source can be a very useful, controllable broadband acoustic sound source.

IV. REFERENCES

1. Page, C. H., Instantaneous Power Spectra, Journal of Applied Physics, 23,
    (1952). p. 103

2. Junger, M. C., Energy Exchange between Incompressible Near and Acoustic Far
    Field for Transient Sources, Journal of the Acoustic Society of America, 40,
    5 (1966). p. 1025

3. Caulfield, D. D., Predicting Sonic Pulse Shapes of Underwater Spark Discharges,
    Woods Hole Oceanographic Institute, Report No. 60-12 (March 1962).

4. Martin, E. A., The Underwater Spark: An Example of Gaseous Conduction at
    About 10,000 Atmospheres, University of Michigan Engineering Research
    Institute, Report 2048-12 (July 1965).

5. Hersey, J. B., S. T. Knott, D. D. Caulfield, H. E. Edgerton, and E. E. Hays,
    Adaptation of Sonar Techniques for Exploring the Sediments and Crust of the
    Earth Beneath the Ocean, Journal of the British Institute of Radio Engineers
    (September 1963). p. 245

DOCUMENT CONTROL DATA - R & D

(Security classification of title, body of abstract and indexing annotation must be entered when the overall report is classified)

1. ORIGINATING ACTIVITY (Corporate author)	2a. REPORT SECURITY CLASSIFICATION
Avco Government Products Group	None
Avco Applied Technology Division	2b. GROUP
Lowell Industrial Park, Lowell, Massachusetts 01851	--

3. REPORT TITLE

Summary Technical Report, The Electrodeless Spark Underwater Sound Source

4. DESCRIPTIVE NOTES (Type of report and inclusive dates)
Contract report

5. AUTHOR(S) (First name, middle initial, last name)

H. A. Wright, Jr.

6. REPORT DATE	7a. TOTAL NO. OF PAGES	7b. NO. OF REFS
8 January 1970	39	5
8a. CONTRACT OR GRANT NO.	9a. ORIGINATOR'S REPORT NUMBER(S)	
Nonr. 4389(00)	AVATD-0200-69-RR	
b. PROJECT NO.		
c.	9b. OTHER REPORT NO(S) (Any other numbers that may be assigned this report)	
d.		

10. DISTRIBUTION STATEMENT

Reproduction in whole or in part is permitted for any purpose of the United States Government. Distribution of this document is unlimited.

11. SUPPLEMENTARY NOTES	12. SPONSORING MILITARY ACTIVITY
	Code 468, Office of Naval Research
	Department of the Navy
	Washington, D. C.

13. ABSTRACT

The electrodeless spark sound source is an impulsive electro-acoustic transducer. It generates a broadband impulse which is typically several tens of microseconds in duration. The electrodeless spark principle is described, and the results of parametric studies presented. It is found that the device is long lived, its emitted pressure waveform can be readily controlled, the emitted waveform is extremely reproducible, and the bubble pulse emission can be virtually eliminated.

The peak pressure developed at one yard is typically a few tenths of a bar to several bars. The electro-acoustic efficiency is modest, usually being no more than a few percent.

A discussion of several specific device configurations shows that the waveform of the emitted pressure is strongly dependent upon both the electric and, particularly, the geometric parameters used.

DD FORM 1473 NOV 65

Security Classification

14 KEY WORDS	LINK A		LINK B		LINK C	
	ROLE	WT	ROLE	WT	ROLE	WT
Electrodeless spark						
Underwater sound source						
Summary technical report						